



HAL
open science

Solar redox cycling of ceria in a monolithic reactor for two-step H₂O/CO₂ splitting: Isothermal methane-induced reduction versus temperature-swing cycle

Anita Haeussler, Srirat Chuayboon, Stéphane Abanades

► To cite this version:

Anita Haeussler, Srirat Chuayboon, Stéphane Abanades. Solar redox cycling of ceria in a monolithic reactor for two-step H₂O/CO₂ splitting: Isothermal methane-induced reduction versus temperature-swing cycle. AIP Conference Proceedings, 2020, pp.170009. 10.1063/5.0028582 . hal-03077551

HAL Id: hal-03077551

<https://hal.science/hal-03077551>

Submitted on 16 Dec 2020

HAL is a multi-disciplinary open access archive for the deposit and dissemination of scientific research documents, whether they are published or not. The documents may come from teaching and research institutions in France or abroad, or from public or private research centers.

L'archive ouverte pluridisciplinaire **HAL**, est destinée au dépôt et à la diffusion de documents scientifiques de niveau recherche, publiés ou non, émanant des établissements d'enseignement et de recherche français ou étrangers, des laboratoires publics ou privés.

Solar redox cycling of ceria in a monolithic reactor for two-step H₂O/CO₂ splitting: Isothermal methane-induced reduction versus temperature-swing cycle

Cite as: AIP Conference Proceedings **2303**, 170009 (2020); <https://doi.org/10.1063/5.0028582>

Published Online: 11 December 2020

Anita Haeussler, Srirat Chuayboon, and Stéphane Abanades



View Online



Export Citation

ARTICLES YOU MAY BE INTERESTED IN

[Technical feasibility of integrating concentrating solar thermal energy in the Bayer alumina process](#)

AIP Conference Proceedings **2303**, 140005 (2020); <https://doi.org/10.1063/5.0029572>

[Analysis of process parameters influence on syngas yields and biomass gasification rates in a continuous particle-fed solar-irradiated gasifier](#)

AIP Conference Proceedings **2303**, 170005 (2020); <https://doi.org/10.1063/5.0028586>



Your Qubits. Measured.

Meet the next generation of quantum analyzers

- Readout for up to 64 qubits
- Operation at up to 8.5 GHz, mixer-calibration-free
- Signal optimization with minimal latency

Find out more



Solar Redox Cycling of Ceria in a Monolithic Reactor for Two-Step H₂O/CO₂ Splitting: Isothermal Methane-Induced Reduction versus Temperature-Swing Cycle

Anita Haeussler¹, Srirat Chuayboon^{1,2}, and Stéphane Abanades^{1,a)}

¹ *Processes, Materials and Solar Energy Laboratory, PROMES-CNRS, 7 Rue du Four Solaire, 66120 Font-Romeu, France*

² *Department of Mechanical Engineering, King Mongkut's Institute of Technology Ladkrabang, Prince of Chumphon Campus, Chumphon 86160, Thailand*

^{a)}Corresponding author: stephane.abanades@promes.cnrs.fr

Abstract. Solar thermochemical cycles provide an efficient route to convert solar energy into valuable chemical energy carriers, such as solar fuels. The splitting of CO₂ and H₂O using metal oxide redox pairs permits to produce clean synthetic fuels. Furthermore, CO₂ is upgraded into a valuable product (CO) that can be further converted to liquid hydrocarbon fuels when combined with H₂. Among the possible candidate materials for two-step redox cycling, ceria appears promising given the high oxygen mobility and exchange property in the crystal lattice offering large amounts of oxygen vacancies (δ in CeO_{2- δ}) while retaining fluorite structure, rapid and reversible transition between Ce⁴⁺ and Ce³⁺ oxidation states, and stable crystal structure during cycling. During a first step at high temperature, the metal oxide (CeO₂) is reduced by releasing O₂ thus creating oxygen vacancies in the ceria structure. In a second step at lower temperature, the non-stoichiometric oxide (CeO_{2- δ}) is re-oxidized with CO₂ or H₂O, leading to the production of CO or H₂ (solar fuels). This temperature-swing operating mode requires high temperatures during the reduction and a temperature gap between the two steps, which impacts the solar-to-fuel efficiency. The use of methane as reducing agent in the reduction step can be used to decrease the reduction temperature and allow isothermal operation. A comparison between the two operating modes, namely isothermal methane-induced reduction versus temperature-swing cycle, was performed in a monolithic solar reactor integrating ceria porous foams. The reduction of ceria using methane results in a higher reduction extent and fuel production with lower cycle temperatures (950-1050°C) at the expense of using a carbonaceous reducer. Thus, the temperature-swing operation appears as a more suitable long-term option for sustainable solar fuel production, but shows more stringent requirements on the reacting materials and solar reactor. The fuel production in the temperature-swing cycle was further increased by decreasing the pressure or increasing the reduction temperature, while the material performance stability was not altered after extended cycling.

INTRODUCTION

Conventional energy production pathways show adverse environmental impacts; therefore, alternative renewable energies should be developed to produce clean energy carriers. Thermochemical cycles using concentrated sunlight for H₂O and CO₂ splitting into fuels is an elegant way to convert and store intermittent solar energy into chemical fuels [1–3]. The solar-driven two-step ceria redox cycle for CO (or H₂) production from CO₂ (or H₂O) dissociation offers clean sustainable renewable fuels. When coupled to the capture of CO₂ from atmospheric air or exhaust combustion gases, the CO production can be considered as carbon neutral. Ceria is considered as a state-of-art material for the thermochemical cycles due to its ability to maintain its crystallographic structure over a large range of non-stoichiometry and operating conditions. On top of that, it shows a thermodynamically favorable and rapid oxidation [4–10].

The first step of the redox cycle is an endothermic reduction at high temperature (Eq. 1) using concentrated solar energy as external heat source. The second step is an exothermic oxidation (Eq. 2) with an oxidant gas (CO₂ or H₂O) at lower temperatures:



The production of CO and H₂ in a solar reactor with ceria as reactive material has been demonstrated [11–14]. Currently, the highest energy efficiency of 5.25% was reached in a monolithic reactor with ceria reticulated foam [15].

However, the major drawbacks of this process are: the high operating temperature requirement that exceeds 1400°C during the reduction step [16], and the temperature swing between reduction and oxidation steps, which in turn adversely results in high sensible heat losses, thereby decreasing solar-to-fuel efficiency.

Alternatively, employing hydrocarbon as reducing agent such as methane (CH₄) in the reduction step can lower the reduction temperature until the cycle can be operated isothermally (both reduction and oxidation steps at ~1000°C), thereby avoiding sensible heat losses [17]. In this case, the reduction reaction can be represented by:



The cycle consists of both endothermic ceria reduction and simultaneous partial methane oxidation (Eq. 3), followed by exothermic reduced ceria oxidation with H₂O/CO₂ (Eq. 2). The main advantages are the isothermal operation, the production of a syngas suitable for methanol synthesis during the reduction, and the absence of costly catalysts for methane reforming.

This study aims to present the influence of operating parameters on the thermochemical performance of a monolithic solar reactor. A comparison between isothermal (using CH₄ for ceria reduction) and temperature-swing cycles is performed.

EXPERIMENTAL SETUP AND METHODS

The experiments were performed using a 1.5 kW_{th} vertical-axis solar facility (composed of a sun-tracking heliostat reflecting sunlight to a facedown parabolic concentrator) at PROMES-CNRS (France). The solar monolithic reactor for the two-step H₂O/CO₂ splitting either performed with reduction step using methane (isothermal) or with temperature-swing operation driven by highly concentrated solar radiation is depicted in Figure 1. The reactive foam (~ 50 g) was placed in a ceramic cavity (alumina) with inner diameter of 50 mm and 80 mm height for temperature-swing cycles. The cavity aperture was positioned at the focal point of the solar concentrator. The incident concentrated solar power was thus absorbed by the cavity after passing through a transparent hemispherical window. Reticulated porous ceria foams with 87% porosity and cylindrical geometry were prepared as reactive oxygen carrier materials via a replication technique using polymer templates [18]. Two foams were tested with different pore size densities: 10 and 20 pores per inch (ppi), designated in the following as 10 ppi and 20 ppi foams. The temperature was monitored at different locations of the reactor thanks to two B-type thermocouples (T1 and T2 as represented on Figure 1) and a solar-blind pyrometer (temperature range: 500-2500°C, wavelength: 5.14 μm) [19], pointing into the cavity through a fluorine window. The cavity pressure was also measured by a pressure sensor. During temperature-swing cycles, the reactor was solar-heated to the desired temperature in pure Ar (1.2 NL/min) to release O₂ (1400-1450°C during thermal reduction) and cooled during oxidation with CO₂ (or H₂O) to produce CO (or H₂) in the 800-1100°C range. The CO₂ flow rate was 0.4 NL/min (25% mole fraction) and H₂O flow rate was 200 mg/min (17% mole fraction). In the reduction step at low pressure, a pump at the reactor outlet was used to decrease the total pressure in the reactor chamber swept continuously with inert gas flow. Concerning isothermal CH₄-induced reduction, another reactive foam with the same porosity was used and experiments were conducted at 950, 1000, and 1050°C while alternating the flow between CH₄ (0.2 NL/min) along with Ar (0.2 NL/min) for reduction step (50% inlet CH₄ mole fraction) and H₂O (200 mg/min) for subsequent oxidation step (55% steam mole fraction at inlet). The produced gases (O₂, H₂, CO for temperature-swing redox cycle and H₂, CO, CO₂, CH₄ for methane-promoted redox cycle) were analyzed at the output thanks to online gas analyzers (electrochemical sensor for O₂, thermal conductivity detector for H₂, and infrared sensors for CO, CO₂, CH₄, calibrated with standard gases). The averaged oxygen nonstoichiometry (δ), fuel yields, gas production rates, and reactor performance were experimentally studied and compared.

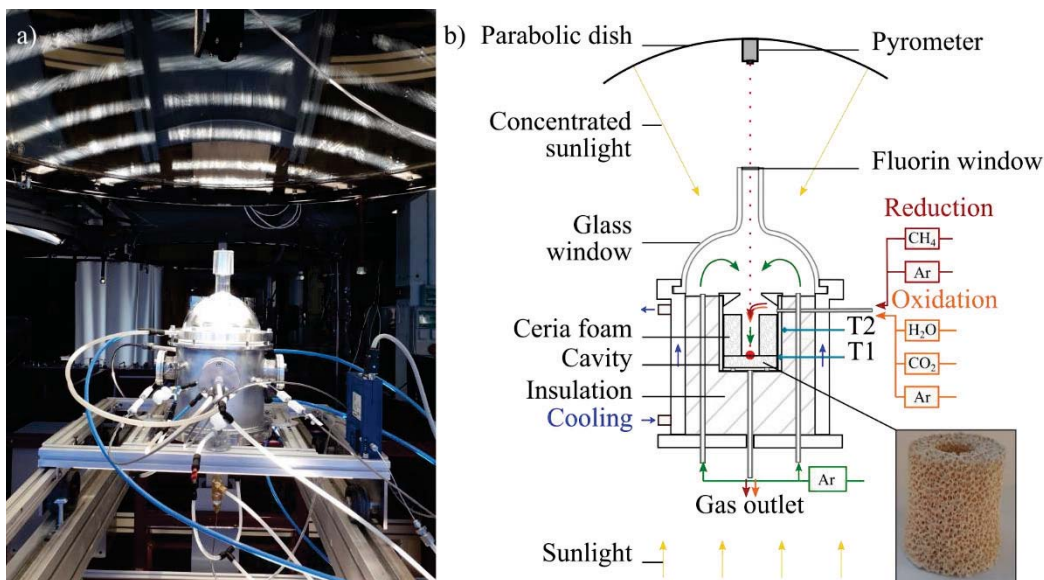


FIGURE 1. a) photography and b) schematic illustration of the ceria redox cycling in a 1.5 kWth monolithic solar reactor driven by real high-flux concentrated sunlight

RESULTS AND DISCUSSION

Temperature-Swing Cycles

Concerning the temperature-swing mode, different parameters, such as the reduction and oxidation temperatures, and the total pressure applied during the reduction, have been investigated in order to optimize the fuel production yield. The influence of the reduction temperature was studied by determining its impact on the O_2 released during reduction and subsequent fuel production during oxidation. Figure 2 presents two cycles performed with different reduction temperatures (1400°C and 1450°C for T1) followed by a non-isothermal re-oxidation with CO_2 (oxidation during natural cooling without any solar power input, CO_2 injection at about 1000°C). O_2 and CO are produced during reduction and oxidation respectively. Their amounts is calculated by integrating the production peaks. Given the slight withdrawal of T2 thermocouple from the cavity to avoid its direct exposure to solar flux, T2 is lower than T1, even if it is located in the upper cavity region where the solar input is maximum. The temperature measured by the pyrometer can be 70°C higher than T1. This highlights a temperature gradient in the foam between the upper part of the foam directly exposed to the solar flux and the bottom part distant from the solar input. A temperature gradient in the foam leads to a non-uniform reduction extent reached in the foam during the reduction step. Therefore the reported non-stoichiometries (δ) calculated in the following are the foam-averaged non-stoichiometries. T1 was considered as the reference temperature in the following to ensure that the whole foam is heated above this temperature. The temperature increase of 50°C during the reduction step (from 1400 to 1450°C) enhanced the O_2 produced by 44 % (103.3 to $139.0 \mu\text{mol/g}$, $\delta=0.036$ to 0.048) then leading to a 15 % increase of the CO amount produced. The peak rate of CO production also increased accordingly. Increasing the reduction temperature thus permits to improve the reduction step, in turn leading to an improved fuel production yield. However it should be kept in mind that the maximum temperature is limited by the reactor materials and the reactive material itself. Higher temperatures may result in materials sintering, losses by sublimation and increased heat losses. Furthermore the increase of the reduction temperature leads to an increase of the temperature swing between both cycle steps, thus favoring heat losses through materials heating/cooling.

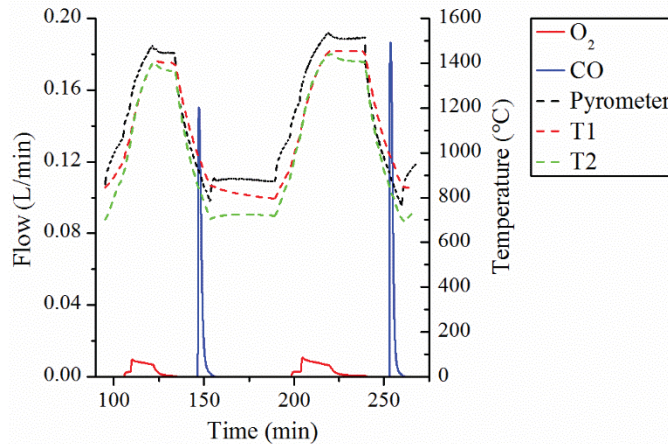


FIGURE 2. O₂ and CO production rates along with reactor temperatures, during consecutive cycles for ceria foam with temperature-swing mode for the 20 ppi foam

The other parameter investigated during the reduction step is the pressure. According to thermodynamics, the oxygen partial pressure directly affects the reduction extent reached at equilibrium by the non-stoichiometric material. The oxygen partial pressure was varied by modifying the total pressure. Two cycles were performed at atmospheric and reduced pressure, respectively, as represented in Figure 3. The decrease of the pressure from 865 hPa to 110 hPa during the reduction leads to an improvement of the reduction extent by an increase of 48% in the oxygen amount produced (86 to 125 $\mu\text{mol/g}$, $\delta=0.030$ to 0.043). Consequently, the increase of the reduction extent is followed by an improvement of the CO production yield from 160 $\mu\text{mol/g}$ to 258 $\mu\text{mol/g}$. However, the energy consumption by pumping leads to energy penalties that must be balanced with the gains in the fuel productivity. A decreased pressure during the reduction step has a beneficial effect on the thermochemical cycling performance as it permits to increase both the oxygen amount produced and the fuel production yield.

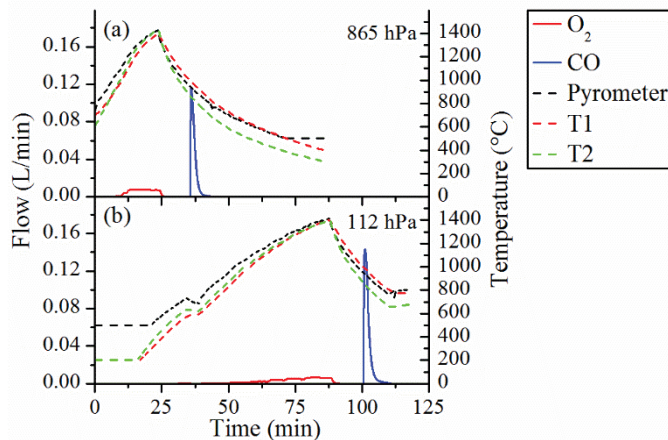


FIGURE 3. O₂ and CO production rates along with reactor temperatures at different pressures during reduction: (a) atmospheric pressure and (b) reduced pressure during the reduction step for the 20 ppi foam

The impact of the oxidation temperature on the fuel production yield was also studied. Figure 4 depicts the O₂ and CO production rates during three cycles with different oxidation temperatures (1160°C, 1050°C and 950°C respectively). During these cycles, the oxidation was performed at a constant temperature, thus requiring solar power input to maintain the temperature. The decrease of the oxidation temperature leads to an increase of the amount of fuel produced along with an increase of the fuel production rate. The CO amount produced increases from 81 to 197 $\mu\text{mol/g}$ when the oxidation temperature decreases by $\sim 200^\circ\text{C}$, because the oxidation reaction is thermodynamically favored when decreasing the temperature. Similarly, the CO maximal production rate shows a 6-fold increase (0.33 to 2.05 $\text{mL.g}^{-1}.\text{min}^{-1}$) when decreasing the re-oxidation temperature from 1160°C to 950°C. The

decrease of the oxidation temperature has a beneficial impact on the oxidation step by improving both the CO yield and the production rate. However the decrease of the oxidation temperature also leads to an increase of the temperature swing between each step, which thus induces additional sensible heat losses.

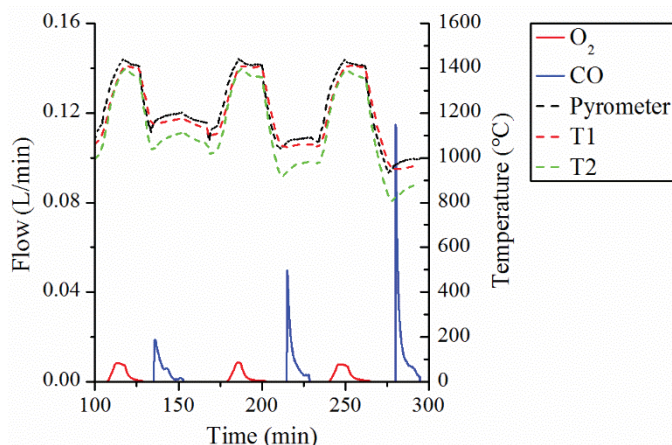


FIGURE 4. Influence of the oxidation temperature during three thermochemical cycles with a reduction temperature of 1400°C followed by an oxidation at 1160°C, 1050°C and 900°C respectively, 20 ppi foam

In the case of non-isothermal oxidation (oxidation during cooling), there is no solar energy input in the reactor and the temperature freely decreases. On the contrary during isothermal oxidation, the reactor is heated to hold constant the temperature. Figure 5 shows the influence of isothermal oxidation (~1050°C) in comparison with non-isothermal oxidation (from 996°C to 847°C) on the fuel production rate. The CO production yield is higher in the non-isothermal mode (260 $\mu\text{mol/g}$) compared with the isothermal mode (121 $\mu\text{mol/g}$). The maximal fuel production rate is almost 3 times higher than the one in isothermal mode. The isothermal oxidation is slow whereas the non-isothermal oxidation reaches completion rapidly. The non-isothermal mode allows a higher fuel production and rate in comparison with isothermal mode without any solar energy input required during the oxidation step. However, after a non-isothermal oxidation with temperature decreasing freely, the temperature swing needed to reach the next reduction step is higher than for isothermal oxidation. Consequently the associated energy input required for heating to the next reduction step is also higher.

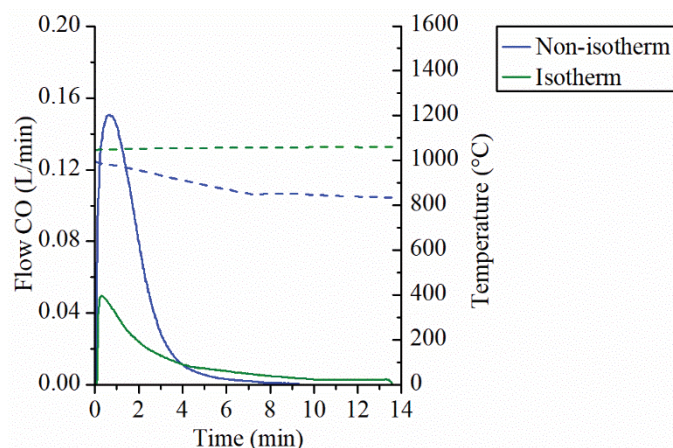


FIGURE 5. CO production rate after a reduction at ~1400°C in isothermal (1050°C) and non-isothermal (996°C to 847°C) oxidation along with the T1 temperature (dotted lines) for the 20 ppi foam

In order to evaluate the impact of the oxidant gas (CO₂ or H₂O) on the reactor performance, different cycles have been performed with CO₂ and H₂O as oxidant gas (Figure 6). For both temperatures presented (1050°C and 900°C), the CO shows higher peak production rate and shorter duration than H₂ production. At ~900°C, the H₂ and CO production are similar (221 and 210 μmol/g, respectively) whereas at ~1050°C the amount of H₂ produced (128 μmol/g) is lower than CO (194 μmol/g). Above ~1000°C, the fuel production is favored with CO₂ as oxidant gas (oxidation with H₂O is less favorable). Under ~1000°C, the fuel production is similar whatever the oxidant gas. However, the CO₂ splitting reaction is faster than water splitting reaction. Therefore water splitting requires a lower oxidation temperature than CO₂ splitting. Decreasing the oxidation temperature to favor the hydrogen production implies further heat losses. However in both cases, the oxidant gas conversion is not complete. The output gas is thus an oxidant/fuel mix which would require being separated in industrial process. Hydrogen can be easily separated from water at room temperature whereas the separation of CO from CO₂ requires additional energy or advanced technologies [7].

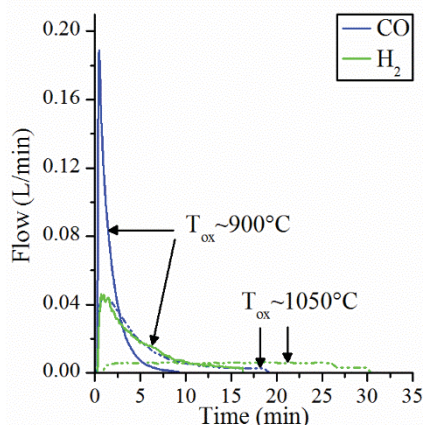


FIGURE 6. CO and H₂ production rates during isothermal oxidation at 1050°C (dotted lines) and 900°C (solid lines)

In summary, concerning the temperature-swing cycle, the increase of the reduction temperature or the decrease of the oxygen partial pressure (by pumping) enhanced the ceria reduction extent, in agreement with thermodynamics. During the oxidation step with CO₂ (or H₂O), the fuel production rate increased when decreasing the oxidation temperature at the expense of a larger temperature swing (inducing heat losses). The highest oxygen non-stoichiometry achieved during reduction (at ~1425°C and pressure of 110 hPa) was $\delta=0.059$. Maximum fuel production during one cycle was 0.302 mmol/g_{CeO₂} (35 cycles performed, 20 ppi foam) with peak fuel production rate of 3.3305 ml.g⁻¹.min⁻¹. The fuel productions from the 10 and 20 ppi foams are summarized in Table 1. In the case of the 10 ppi foam, cycles 3, 4, 10, 14 and 17 were performed with similar operatory conditions ($T_{red}\sim 1400^\circ\text{C}$, $T_{ox}\sim 1040^\circ\text{C}$), and the fuel production showed good stability over cycles. The pore size of the foam does not show any significant impact on the fuel production amount. For example, the CO amount produced in average per cycle for the 10 and 20 ppi foams are 4.33 L/kg_{CeO₂} and 4.97 L/kg_{CeO₂} respectively. In total, the 10 ppi and 20 ppi foams produced 3.31 L and 2.78 L of CO respectively (during 14 and 10 cycles, respectively). The H₂ produced by the 10 and 20 ppi foams reached 0.68 L and 1.10 L respectively (during 3 and 4 cycles respectively). Each foam successfully underwent ~30h of continuous on sun operation without any significant performance decline, demonstrating their good thermal stability.

TABLE 1. Summary of the fuel production with operatory conditions for 10 ppi and 20 ppi foams, * indicates a low pressure of ~110 hPa during the reduction step

Cycle	Foam	Reduction / oxidation temperatures (°C)	Oxidant gas	O ₂ production (μmol/g)	Fuel production (μmol/g)
1	10 ppi	1378 / 967	H ₂ O	105	208
2	10 ppi	1417 / 1006	H ₂ O	109	216
3	10 ppi	1404 / 1034	CO ₂	106	213
4	10 ppi	1407 / 1032	CO ₂	97	188
5	10 ppi	1400 / 1079	CO ₂	107	212
6	10 ppi	1412 / 1114	CO ₂	88	120
7	10 ppi	1407 / 1121	CO ₂	84	161
8	10 ppi	1380* / 907	CO ₂	102	203
9	10 ppi	1408 / 1213	CO ₂	115	136
10	10 ppi	1408 / 1059	CO ₂	98	194
11	10 ppi	1453 / 1050	CO ₂	116	226
12	10 ppi	1404 / 869	CO ₂	98	197
13	10 ppi	1403 / 1011	CO ₂	78	151
14	10 ppi	1405 / 1055	CO ₂	86	152
15	10 ppi	1402 / 954	CO ₂	96	191
16	10 ppi	1458 / 1061	CO ₂	119	237
17	10 ppi	1405 / 1057	H ₂ O	77	129
1	20 ppi	1410 / 1064	CO ₂	110	186
2	20 ppi	1408 / 1162	CO ₂	67	81
3	20 ppi	1411 / 1056	CO ₂	60	121
4	20 ppi	1409 / 955	CO ₂	87	197
5	20 ppi	1412 / 1053	H ₂ O	95	118
6	20 ppi	1401 / 870	H ₂ O	90	250
7	20 ppi	1410 / 903	CO ₂	106	210
8	20 ppi	1410 / 705	CO ₂	118	273
9	20 ppi	1424* / 1048	CO ₂	174	296
10	20 ppi	1407 / 858	H ₂ O	108	222
11	20 ppi	1409 / 1000→844	CO ₂	123	261
12	20 ppi	1407 / 996→847	CO ₂	126	260
13	20 ppi	1456 / 997→845	CO ₂	149	302
14	20 ppi	1454 / 1004→673	H ₂ O	135	266

Isothermal Cycles with CH₄-Induced Reduction

On-sun experiments were performed with another reactive foam (18.37g, 10 ppi) for twelve consecutive cycles at 950 °C (1 cycle), 1000 °C (10 cycles) and 1050 °C (1 cycle) in order to investigate the isothermal cycles with CH₄-induced reduction. When employing CH₄ as reducing agent, the cycle was operated isothermally, avoiding the heat losses associated with temperature swing between reduction and oxidation steps as described before. Figure. 7 shows the representative transient production rates (from cycle #2) of syngas along with nominal reactor temperature (corresponding to T1) during ceria endothermic reduction with methane, followed by exothermic ceria oxidation with H₂O at 1000 °C. During reduction step (Figure 7a), at the beginning of reaction the formation of both CO₂ and H₂O (not measured) is attributed to the excess of oxygen at ceria surface reacting with CH₄, and the reactor temperature drop is due to the endothermic reaction. H₂ and CO production rates increased significantly (H₂/CO molar ratio approaching two), while CH₄ was concomitantly consumed. The syngas then decreased progressively after completing ceria reduction. When the CO production rate approached zero, the CH₄ flow was subsequently stopped. During subsequent oxidation (Figure 7b), at initial stage the temperature increased slightly as a result of exothermal reaction;

meanwhile, H₂ increased sharply while a small CO production rate was first observed, followed by CO₂, arising from the gasification of carbon deposition (stemming from CH₄ cracking in the first step). The final obtained H₂, CO, and CO₂ yields (calculated by time-integration of the measured syngas production rates produced per gram of CeO₂) were 3.83, 1.74, and 0.10 mmol/g_{CeO₂} in the reduction step and 2.24, 0.13, and 0.02 mmol/g_{CeO₂} in the oxidation step, respectively. The δ at both the reduction and oxidation step was found to be very similar ($\delta_{\text{red}}=0.37$ and $\delta_{\text{ox}}=0.36$), thereby confirming complete ceria oxidation. In this test, the methane conversion, solar-to-fuel energy conversion efficiency, and energy upgrade factor (their expressions were defined in [17]) of 56.8%, 3.9%, and 1.0, respectively, were accomplished. This thus outperforms the temperature-swing cycle in terms of higher $\eta_{\text{solar-to-fuel}}$ thanks to employing methane that dramatically lowers the reduction temperature and associated heat losses, in turn improving the $\eta_{\text{solar-to-fuel}}$.

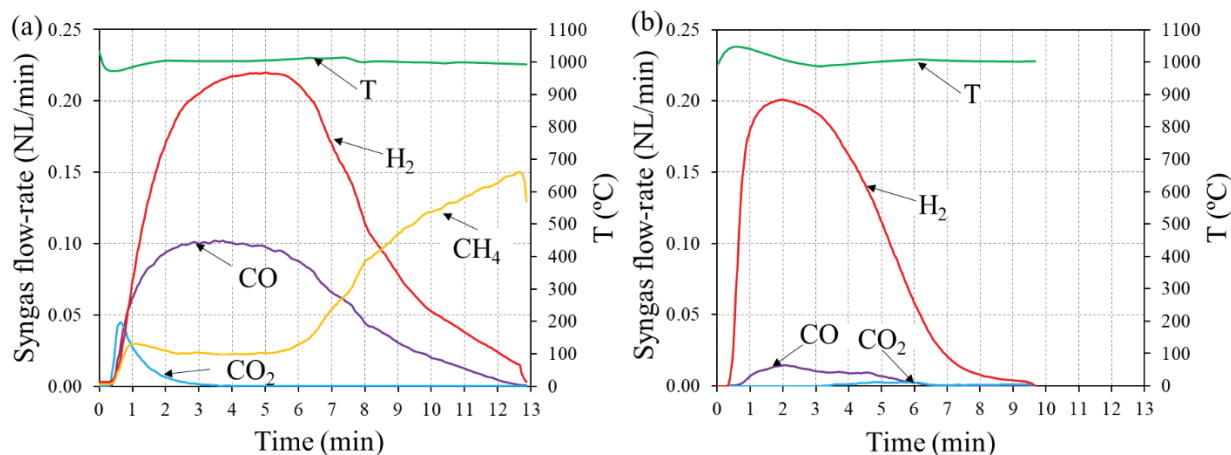


FIGURE 7. Syngas production rate along with reactor temperature T1 for (a) reduction with CH₄ and (b) oxidation with H₂O of ceria foam cycled isothermally at 1000 °C.

In order to demonstrate ceria cycling stability during isothermal cycles with CH₄-induced reduction, the syngas yields during ceria reduction with methane (Figure. 8a), followed by ceria oxidation with H₂O (Figure. 8b) is plotted for twelve successive runs. These syngas yields were quantified separately, segregating the gases produced from the main reactions regarding both partial reduction of ceria by methane (Eq. 3) and ceria oxidation (Eq. 2), and from the side reactions regarding both the H₂ produced by methane cracking (CH₄→2H₂+C) and the gases produced from C deposit gasification with steam during oxidation (C+H₂O→CO+H₂, and C+2H₂O→CO₂+2H₂). A stable pattern in the H₂ (CeO₂+CH₄), CO(CeO₂+CH₄), and CO₂(CeO₂+CH₄) yields over the ten cycles at 1000 °C was achieved, in the ranges 3.48-3.64 mmol/g_{CeO₂} for H₂ (CeO₂+CH₄), 1.74-1.82 mmol/g_{CeO₂} for CO(CeO₂+CH₄), and 0.07-0.10 mmol/g_{CeO₂} for CO₂(CeO₂+CH₄) (Figure 8a), in turn resulting in stable total syngas yield (5.67-6.80 mmol/g_{CeO₂}), δ_{red} (0.35-0.38), and X_{CH₄} evolution profile (46.9-60.9%, Figure 9). The H₂(CH₄ cracking) yield at 1000 °C fluctuated slightly (in the range 0.35-1.27 mmol/g_{CeO₂}) because of a small difference in the CH₄ injection duration [20]. Note that the H₂(CH₄ cracking) was quantified by the total H₂ yield measured by gas analysis minus the H₂ yield produced by the reaction of ceria with methane, which is equivalent to twice the quantity of produced CO, according to Eq. 3. When either increasing or decreasing the temperature (1050 °C at cycle #5 or 950 °C at cycle #6), the total syngas yield varied significantly because of a change in the reaction kinetics. The maximum total syngas yield (7.48 mmol/g_{CeO₂}) was consequently found at the maximum temperature (1050 °C), demonstrating kinetic rate improvement (Figure 10). The logarithm evolution of the reaction rates versus inverse temperature ($k = A \cdot \exp(-E_a/RT)$) was plotted in Figure 10 to determine the activation energy (E_a) of the ceria reduction process. The reaction rate constants (k) were quantified from the peak production rates of H₂ and CO at 950 °C (cycle #6), 1000 °C (cycle #4), and 1050 °C (cycle #5). As a result, the slope of ln k for both H₂ and CO production rates increased linearly with the inverse temperature. The E_a values were 114.2 kJ/mol for H₂ and 93.4 kJ/mol for CO. The E_a value related to H₂ production rates was slightly higher compared to that of CO as a result of the side reaction effect attributed to CH₄ cracking. This side reaction produces additional H₂ and thus modifies the global H₂ production rate arising only from the reaction with ceria. In contrast, CO is only produced from methane reforming (Eq. 3) and better represents the kinetics of ceria reduction reaction. Moreover, the H₂ (CH₄ cracking) yield was negligible at 900 °C, in agreement with the lowest X_{CH₄} (20%); in contrast, it was maximal (2.0 mmol/g_{CeO₂}) at the highest temperature (1050 °C) in agreement with the

highest X_{CH_4} (65.9%), thereby indicating that the extent of CH_4 cracking reaction is strongly dependent on the temperature [21]. For isothermal cycles with CH_4 -induced reduction, a temperature trade-off at 1000 °C is recommended to hasten the kinetic rate of ceria reduction while alleviating the side reaction associated with CH_4 cracking.

Concerning oxidation (Figure 8b), the H_2 ($CeO_{2-\delta}+H_2O$) yield was stable at 1000 °C (in the range 2.04-2.17 mmol/ g_{CeO_2}), except for cycles #5 and #6 caused by the different temperature during the reduction step and its impact on the reduction extent. Likewise, the H_2 (C+ H_2O), H_2 (C+2 H_2O), CO(C+ H_2O), and CO_2 (C+ H_2O) yields at 1000 °C were fairly constant in negligible amounts (0.11-0.18, 0.04-0.10, 0.11-0.18, and 0.02-0.05 mmol/ g_{CeO_2} , respectively). Note that the H_2 (C+ H_2O) yield is equal to the CO yield measured by gas analysis ($C+H_2O \rightarrow CO+H_2$), while the H_2 (C+2 H_2O) yield is equal to twice the CO_2 yield measured by gas analysis ($C+2H_2O \rightarrow CO_2+2H_2$). The total syngas yield was in the range 2.38-2.57 mmol/ g_{CeO_2} , and δ_{ox} was in the range 0.35-0.37 (consistent with δ_{red}) (Figure 9). Thus, the cycling stability of ceria in the isothermal cycles with CH_4 -induced reduction was validated with respect to stable patterns in produced syngas, δ , and X_{CH_4} .

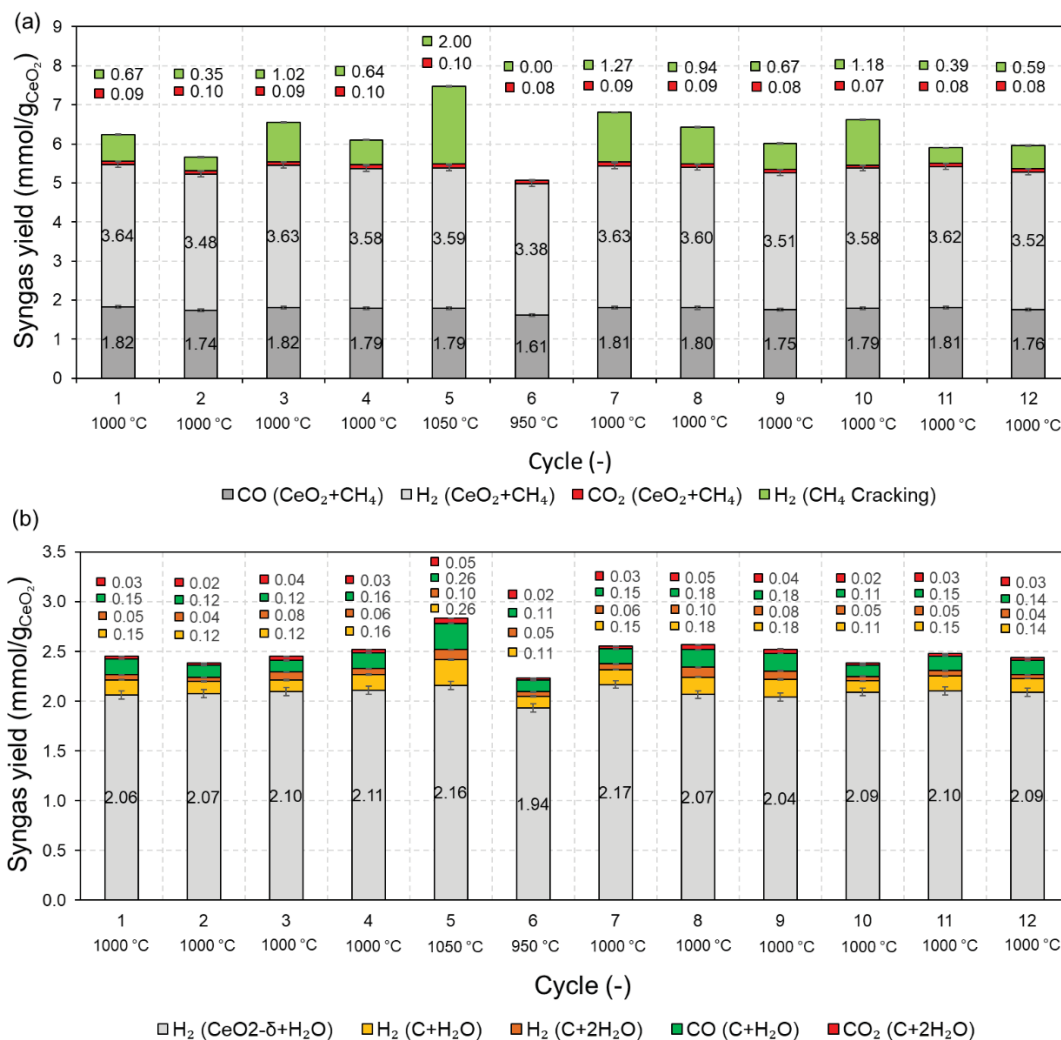


FIGURE 8. Syngas yields for both reduction and re-oxidation of ceria porous foam during 12 consecutive redox cycles performed isothermally.

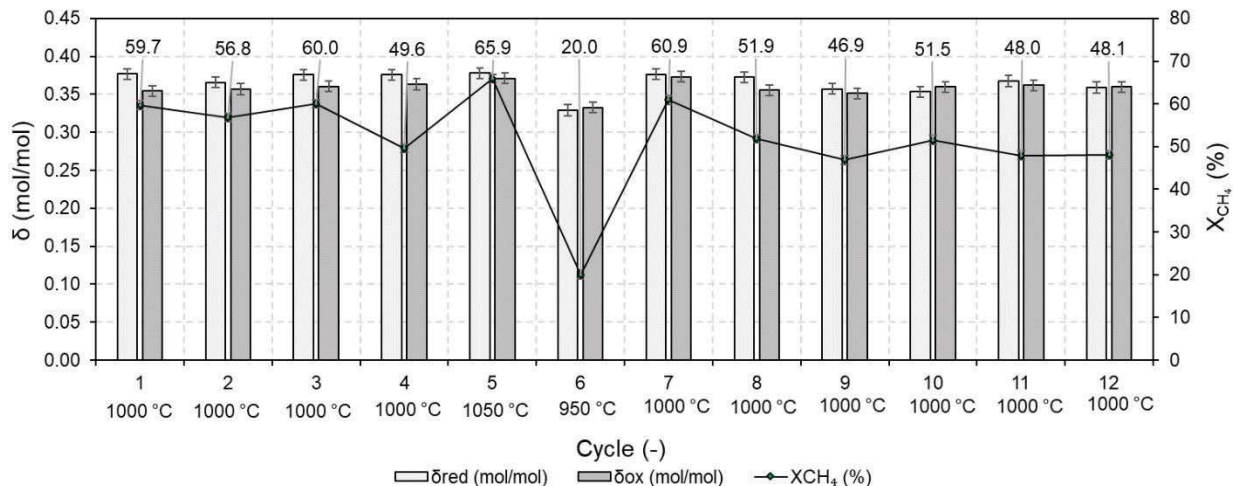


FIGURE 9. Comparison of δ_{red} and δ_{ox} in ceria along with CH_4 conversion during 12 consecutive redox cycles performed isothermally.

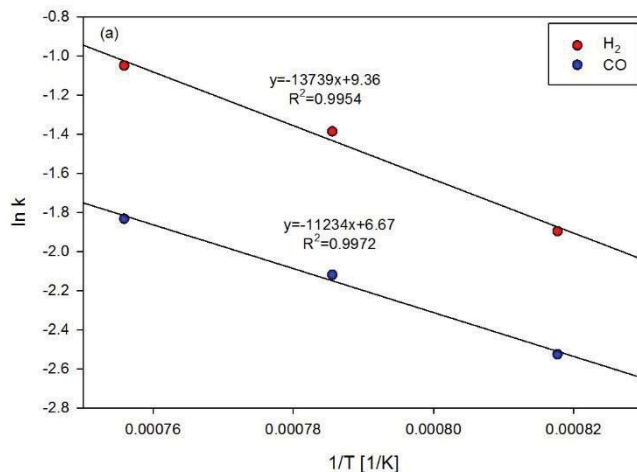


FIGURE 10. Arrhenius plot for H_2 and CO production rates in the range 950-1050 °C during ceria foam reduction.

CONCLUSION

The thermochemical performance of a solar monolithic reactor integrating ceria oxygen carrier for H_2O or CO_2 splitting has been experimentally investigated. In the temperature-swing mode, the reduction extent, and the fuel production yield can be improved by increasing the reduction temperature and/or decreasing the total pressure (oxygen partial pressure) during the reduction step. A decrease of the oxidation temperature improves the oxidation rate. Hence, both the fuel yield and production rate can be enhanced with a decrease of the oxidation temperature or with a non-isothermal oxidation (free cooling with no solar input), although also increasing the temperature swing and inducing heat losses. In total the solar reactor was run over 60h during continuous on sun operation with total production of 1.77 L and 6.09 L of H_2 and CO , respectively and good performance stability.

Furthermore, a comparison between temperature-swing and isothermal cycle (using methane as reducer) has been successfully performed. The reduction extent reached by ceria is higher ($\delta=0.33-0.37$) when methane is used during the reduction. Ceria reduction extent and fuel production yields are about 6 to 10 times higher when employing CH_4 as reducer at 1000°C, when compared to thermal reduction in Ar at 1400°C. Employing CH_4 in the reduction step

eliminates the sensible heat losses due to reactor cooling, thus in turn enhancing solar-to-fuel efficiency. However, it comes at the expense of CH₄ cracking side reaction leading to carbon deposition that can be gasified with H₂O/CO₂ in the oxidation step. A temperature of 1000 °C is recommended for isothermal cycles with CH₄-induced reduction to limit methane cracking reaction while enabling fast enough reaction kinetics. The CH₄-induced reduction represents an attractive option for the short-term solar process implementation, while temperature-swing cycle eliminates the need for carbonaceous reducer and thus represents the most promising option in the long-term for sustainable fuel production.

REFERENCES

1. A. Steinfeld and R. Palumbo. Solar Thermochemical Process Technology. In *Encyclopedia of Physical Science and Technology*, (R. A. Meyers, Tarzana, 2003), pp.237–256
2. C. Falter and R. Pitz-Paal. *Sol. Energy*, **176**, pp.230–240, (2018)
3. R.J. Carrillo and J.R. Scheffe. *Sol. Energy*, **156**, pp.3–20, (2017)
4. A. Haeussler, S. Abanades, J. Jouannaux, M. Drobek, A. Ayril and A. Julbe. *AIMS Mater. Sci.*, **6**, pp.657–684, (2019)
5. W.C. Chueh and S.M. Haile. *Philos. Trans. R. Soc. Math. Phys. Eng. Sci.*, **368**, pp.3269–3294, (2010)
6. N. Gokon, S. Sagawa and T. Kodama. *Int. J. Hydrog. Energy*, **38**, pp.14402–14414, (2013)
7. C.L. Muhich, S. Blaser, M.C. Hoes and A. Steinfeld. *Int. J. Hydrog. Energy*, **43**, pp.18814–18831, (2018)
8. Y. Hao and A. Steinfeld. *Sci. Bull.*, **62**, pp.1099–1101, (2017)
9. S. Abanades, A. Legal, A. Cordier, G. Peraudeau, G. Flamant and A. Julbe. *J. Mater. Sci.*, **45**, pp.4163–4173, (2010)
10. E. Koepf, S. Zoller, S. Luque, M. Thelen, S. Brendelberger, J. González-Aguilar, M. Romero and A. Steinfeld. “Liquid fuels from concentrated sunlight” *SOLARPACES 2018*, **2126**, (AIP Conference Proceedings, Casablanca, Morocco, 2019), p.180012
11. W.C. Chueh, C. Falter, M. Abbott, D. Scipio, P. Furler, S.M. Haile and A. Steinfeld. *Science*, **330**, pp.1797–1801, (2010)
12. P. Furler, J.R. Scheffe and A. Steinfeld. *Energy Environ. Sci.*, **5**, pp.6098–6103, (2012)
13. I. Ermanoski, N.P. Siegel and E.B. Stechel. *J. Sol. Energy Eng.*, **135**, p.031002, (2013)
14. R. Bader, R. Bala Chandran, L.J. Venstrom, S.J. Sedler, P.T. Krenzke, R.M. De Smith, A. Banerjee, T.R. Chase, J.H. Davidson and W. Lipinski. *J. Sol. Energy Eng.*, **137**, p.031007, (2015)
15. D. Marxer, P. Furler, M. Takacs and A. Steinfeld. *Energy Environ. Sci.*, **10**, pp.1142–1149, (2017)
16. S. Abanades and G. Flamant. *Sol. Energy*, **80**, pp.1611–1623, (2006)
17. S. Chuayboon, S. Abanades and S. Rodat. *Chem. Eng. J.*, **356**, pp.756–770, (2019)
18. S. Karl and A.V. Somers. United States. US3090094A. May 21, 1963.
19. D. Hernandez, G. Olalde, J.M. Gineste and C. Gueymard. *J. Sol. Energy Eng.*, **126**, pp.645–653, (2004)
20. S. Chuayboon, S. Abanades and S. Rodat. *J. Energy Chem.*, **41**, pp.60–72, (2020)
21. S. Chuayboon, S. Abanades and S. Rodat. *Energy Technol.*, p.1900415, (2019)